

A new global potential energy surface of the ground state of $SiH_2^+(X^2A_1)$ system and dynamics calculations of the $Si^+ + H_2$ (v_0=2, j_0=0) → $SiH^+ + H$ reaction

Yong Zhang(张勇), Xiugang Guo(郭秀刚), and Haigang Yang(杨海刚)
Citation: Chin. Phys. B, 2022, 31 (**11**): 113101. DOI: 10.1088/1674-1056/ac7456

What follows is a list of articles you may be interested in

Dynamics of the $Au+H_2$ reaction by time-dependent wave packet and quasi-classical trajectory methods

Yong Zhang(张勇), Chengguo Jiang(姜成果)
Chin. Phys. B, 2019, 28 (**12**): 123101. DOI: 10.1088/1674-1056/ab52f2

Ab initio investigation of excited state dual hydrogen bonding interactions and proton transfer mechanism for novel oxazoline compound

Yu-Sheng Wang(王玉生), Min Jia(贾敏), Qiao-Li Zhang(张巧丽), Xiao-Yan Song(宋晓燕), Da-Peng Yang(杨大鹏)
Chin. Phys. B, 2019, 28 (**10**): 103105. DOI: 10.1088/1674-1056/ab4042

Reaction mechanism of $D+ND \rightarrow N+D_2$ and its state-to-state quantum dynamics

Ting Xu(许婷), Juan Zhao(赵娟), Xian-Long Wang(王宪龙), Qing-Tian Meng(孟庆田)
Chin. Phys. B, 2019, 28 (**2**): 023102. DOI: 10.1088/1674-1056/28/2/023102

Density function theoretical study on the complex involved in Th atom-activated C-C bond in C_2H_6

Qing-Qing Wang(王青青), Peng Li(李鹏), Tao Gao(高涛), Hong-Yan Wang(王红艳), Bing-Yun Ao(敖冰云)
Chin. Phys. B, 2016, 25 (**6**): 063102. DOI: 10.1088/1674-1056/25/6/063102

Accurate double many-body expansion potential energy surface of $HS_2(A^2A')$ by scaling the external correlation

Lu-Lu Zhang(张路路), Yu-Zhi Song(宋玉志), Shou-Bao Gao(高守宝), Yuan Zhang(张媛), Qing-Tian Meng(孟庆田)
Chin. Phys. B, 2016, 25 (**5**): 053101. DOI: 10.1088/1674-1056/25/5/053101

A new global potential energy surface of the ground state of $SiH_2^+(X^2A_1)$ system and dynamics calculations of the $Si^+ + H_2$ ($v_0 = 2$, $j_0 = 0$) $\rightarrow SiH^+ + H$ reaction

Yong Zhang(张勇)[1,†], Xiugang Guo(郭秀刚)[2], and Haigang Yang(杨海刚)[1]

[1] *Department of Physics, Tonghua Normal University, Tonghua* 134002, *China*
[2] *Weifang University of Science and Technology, Shouguang* 262700, *China*

(Received 15 April 2022; revised manuscript received 20 May 2022; accepted manuscript online 29 May 2022)

A global potential energy surface (PES) of the ground state of SiH_2^+ system is built by using neural network method based on 18223 *ab initio* points. The topographic properties of PES are presented and compared with previous theoretical and experimental studies. The results indicate that the spectroscopic parameters obtained from the new PES are in good agreement with the experimental data. In order to further verify the validity of the new PES, a test dynamics calculation of the $Si^+ + H_2$ ($v_0 = 2$, $j_0 = 0$) $\rightarrow H + SiH^+$ reaction has been carried out by using the time-dependent wave packet method. The integral cross sections and rate constants are computed for the title reaction. The reasonable dynamical behavior indicates that the newly constructed PES is suitable for relevant dynamics investigations.

Keywords: potential energy surface, integral cross section, rate constant, time-dependent wave packet

PACS: 31.50.–x, 34.50.Lf, 34.50.–s **DOI:** 10.1088/1674-1056/ac7456

1. Introduction

The $Si^+ + H_2$ reaction as one of ion–molecule reactions was received relatively less attention when compared with other reactions, such as $O^+ + H_2$ and $C^+ + H_2$.[1–4] However, the studies of the $Si^+ + H_2$ reaction and its reverse reaction are of great practical significance, because the SiH^+ ion is postulated as an intermediate specie in the manufacturing process of amorphous silicon films in chemical vapor deposition process.[5–7] Furthermore, the $Si^+ + H_2$ reaction and its reverse reaction are of considerable interest in astrophysics and spectroscopy. For example, the SiH radical and SiH^+ ion have been observed in the Sun's photosphere.[8,9] Therefore, the spectroscopic and dynamics information of SiH_2 and SiH_2^+ systems are very important for the modeling of star atmospheres.

Since Curtis and co-workers[10] reported the $\tilde{A}^2B_1(\Pi) \leftarrow \tilde{X}^2A_1$ transition electronic spectrum of SiH_2^+ ion by using laser photofragment spectroscopy in 1985, numbers of theoretical studies have been carried out. The $\tilde{X}^2A_1$ and $\tilde{A}^2B_1$ potential energy surfaces (PESs) of SiH_2^+ ion in collinear geometries have been reported by Hirst *et al.*[11] in 1986. Later, González *et al.*[12] also presented a new PES in $C_{\infty v}$ and C_{2v} symmetry and the $Si^+ + H_2 \rightarrow SiH^+ + H$ reaction was studied. The PESs of four lowest electronic states of the SiH_2^+ system was constructed by Mort and co-workers[13,14] in 1994. The conical intersection between ground state and excited state has been found and the influence of conical intersection on the photodissociation dynamics has been discussed. In the same year, the three-dimensional potential energy functions of $\tilde{X}^2A_1$ and $\tilde{A}^2B_1$ states of the SiH_2^+ system were reported by Bauer *et al.*[15] and rovibronic spectrum of the SiH_2^+ ion was calculated and compared with experimental values. In 2019, a new global PES for the ground state of the SiH_2^+ system was constructed by Gao *et al.*[16] with the many-body expansion method. In addition, the $H + SiH^+ \rightarrow Si^+ + H_2$ reaction has been studied by using Chebyshev quantum wave packet method based on the new PES. The reaction probabilities, integral cross sections (ICSs) and the rate constants were reported in their work. Later, Zhao *et al.*[17] recalculated the $H + SiH^+ \rightarrow Si^+ + H_2$ reaction based on Gao's PES.[16] In their work, the Chebyshev quantum wave packet method is used and the full Coriolis coupling effect is considered. The reaction probabilities, ICSs and rate constants were reported and the results indicated that the Coriolis coupling has large effect on the final dynamical results.

As discussed above, much less effort has been made in the construction of global PES and related dynamics calculation. The aim of present work is to construct a new global PES for the ground state of the SiH_2^+ system. In order to verify the validity of the new PES, a test dynamics calculation of the $Si^+ + H_2$ ($v_0 = 2$, $j_0 = 0$) $\rightarrow H + SiH^+$ reaction will be carried out based on the new PES. In this paper, the methods used in the *ab initio* calculation, fitting processes and dynamics calculation are shown in Section 2. The topographical features of the PES are presented in Section 3 as well as the dynamical results. The conclusions are displayed in Section 4.

†Corresponding author. E-mail: victor0536@163.com

© 2022 Chinese Physical Society and IOP Publishing Ltd

2. Potential energy surface

2.1. *Ab initio* calculations

The *ab initio* calculations are carried out with MOLPRO software package[18] and the C_s symmetry is used for all configurations. In the *ab initio* calculation, the aug-cc-pVQZ basis set[19,20] for H atom and cc-pwCVQZ[21] basis set for Si atom and an internally contracted multi-reference configuration interaction (MRCI)[22] method is used. In detail, we first perform the state-averaged complete active space self-consistent field (SA-CASSCF)[23,24] calculations over three electronic states (two ^{2}A$'$ and one ^{2}A$''$) with equal weight. In addition, 15 valence electrons of the SiH_2^+ system were involved 13 active orbitals ($11a' + 2a''$). In detail, the 1s, 2s, and 2p orbitals of Si^+ are closed which related to the 4a$'$ and 1a$''$. The active orbitals 7a$'$ and 1a$''$ were mainly contributed by 1s orbital of H and 3s, 3p orbitals of Si^+, while the 2s orbital of H and 4s orbital of Si^+ occupied a relatively small weight. Then, the MRCI calculations were performed with the reference orbitals which provided by the SA-CASSCF calculation. Finally, a total of 21530 *ab initio* points was calculated. In fitting process, the *ab initio* points about 10 eV larger than the minimum potential energy were abandoned and 18223 *ab initio* points were used to construct the PES. The Jacobi coordinates (R_Q, R_{HH}, α) were used to sample the *ab initio* points. R_Q is the distance between Si^+ ion and the midpoint of H_2 molecule. R_{HH} is the bond length of H_2 molecule and α is the angle between R_Q and R_{HH}. In detail, 1.0 Bohr $\leq R_Q \leq$ 25.0 Bohr, 0.6 Bohr $\leq R_{HH} \leq$ 25.0 Bohr, and $1^\circ \leq \alpha \leq 89^\circ$.

2.2. PES fitting

The permutation invariant polynomial neural network (PIP-NN)[25,26] method is adopted in this work, which is widely used in the PES construction such as BrH_2,[27] KH_2,[28] and LiH_2[29] system. To avoid the discontinuities of the derivatives around the boundary, PIP method is used to transform the three bond lengths of the SiH_2^+ system. In detail, $G_1 = (P_{SiH_a^+} + P_{SiH_b^+})/2$, $G_2 = P_{SiH_a^+} \cdot P_{SiH_b^+}$, $G_3 = P_{HH}$, where $P_{SiH_a^+} = \exp(-0.2 \cdot R_{SiH_a^+})$, $P_{SiH_b^+} = \exp(-0.2 \cdot R_{SiH_b^+})$, and $P_{HH} = \exp(-0.2 \cdot R_{HH})$, respectively. In the fitting process, G_1, G_2, and G_3 are used as the input term and two hidden layers are used, each of which involves 15 neurons. The neural network expansion can be written as

$$V_{SiH_2^+} = \sum_{k=1}^{15} w_k^3 \cdot f^2 \left(\sum_{j=1}^{15} w_j^2 \cdot f^1 \cdot \left(\sum_{i=1}^{N_{tot}} w_i^1 \cdot G_i + b_j^1 \right) + b_k^2 \right) + b_1^3, \quad (1)$$

where N_{tot} is the number of energy points, w_i^1, w_j^2 and w_k^3 are the connection weights, b_1^3, b_k^2 and b_j^1 are biases, f^1 and f^2 are training functions.

Over-fitting has always been a problem of neural network. To deal with this problem, the input data are randomly divided into three parts, namely, training part (90%), testing part (5%) and validation part (5%). The root means square error (RMSE) is used to test the accuracy of PES and it can be presented as

$$\mathrm{RMSE} = \sqrt{\frac{1}{N} \sum_{i=1}^{N} \left(y_i^{\mathrm{output}} - y_i^{ab} \right)^2}, \quad (2)$$

where N is the total number of energy points, y_i^{output} is the fitting value and y_i^{ab} is the value of *ab initio* calculation. In this work, the fitting error is only 1.83 meV.

2.3. Topographical features of the potential energy surface

To test the accuracy of PES, the spectroscopic parameters of $SiH^+(X^1\Sigma^+)$ ion and $H_2(X^1\Sigma_g^+)$ molecule obtained from the PES are compared with available theoretical[16] and experimental[30,31] values and the results are shown in Table 1.

Table 1. The spectroscopic constants of the SiH^+ ($X^1\Sigma^+$) and H_2 ($X^1\Sigma_g^+$) molecules.

	R_e (Bohr)	ω_e (cm^{-1})	$\omega_e x_e$ (cm^{-1})	α_e (Bohr)	β_e (Bohr)	D_e (eV)
SiH^+ ($X^1\Sigma^+$)						
This work	2.8440	2142.58	36.61	0.2181	7.6485	3.389
Theo.[16]	2.8482					3.4174
Exp.[30]	2.8423	2157.17	34.24	0.2096	7.6603	3.304
Exp.[31]		2157.15	34.23	0.2015	7.6576	3.374
H_2 ($X^1\Sigma_g^+$)						
This work	1.401	4399.18	129.79	3.2136	60.85	4.726
Theo.[16]	1.401					4.745
Exp.[30]	1.401	4401.21	121.33	3.062	60.85	4.746

As shown in Table 1, the spectroscopic constants obtained from the PES are in good agreement with experimental data. For the SiH^+ ($X^1\Sigma^+$) ion, the bond length, harmonic vibrational frequency, and dissociation energy obtained from the PES deviate from the experimental values by 0.0017 Bohr, 14.57 cm^{-1}, and 0.015 eV, respectively. It is very clear that present values closer to the experimental data than the results reported by Gao *et al.*[16] For the H_2 molecule, the bond length is same with experimental data, the harmonic vibrational frequency lower than the experimental data by about 2 cm^{-1}, and

the dissociation energy is lower than the experimental data by 0.02 eV. As a whole, present PES can give a good description for the two-body term.

The major topographical features of the newly constructed PES are shown in Figs. 2(a) and 2(b), which correspond to the global minimum and vertically approaching geometries, respectively. It is very clear that present PES shows a smooth and correct behavior over the configuration space studied. Figure 2(a) shows the contour plot for the bending angle fixed at 119.73°. Clearly, only a deep potential well is observed and no potential barrier is found. In addition, Fig. 2(a) shows a symmetrical behavior which can be attributed to the exchange symmetry of H atom. Figure 2(b) exhibits the contour plot for the Si^+ ion approach the H_2 molecule in the C_{2v} symmetry. Two potential wells are found which correspond to a local minimum and global minimum geometries, respectively. In addition, a potential barrier is also found.

To make a comparison with available theoretical and experimental results, the spectroscopic parameters of theses stationary points are presented in Table 2 as well as the values obtained from previous theoretical and experimental studies. As shown in Table 2, the global minimum is located at $R_{HH} = 4.8400$ Bohr, $R_{SiH_a^+} = 2.8008$ Bohr, $R_{SiH_b^+} = 2.8008$ Bohr, and $\theta_{[HSiH]^+} = 119.73°$, which is in good agreement with experimental data $R_{HH} = 4.8529$ Bohr, $R_{SiH_a^+} = 2.8161$ Bohr, $R_{SiH_b^+} = 2.8161$ Bohr, and $\theta_{[HSiH]^+} = 119°$. The recently reported PES by Gao *et al.*[16] obtained similar results with ours, both of which are in good agreement with experimental data. For the harmonic vibrational frequency, the ω_{sym} and ω_{asym} are in good agreement with each other, except for the ω_{bend}. For the local minimum, present values are in good agreement with the values reported by Gao *et al.*[16] for both geometric structures and harmonic vibrational frequencies. However, in the transition state, great discrepancies can be found between present values and the results obtained from Gao *et al.*[16]

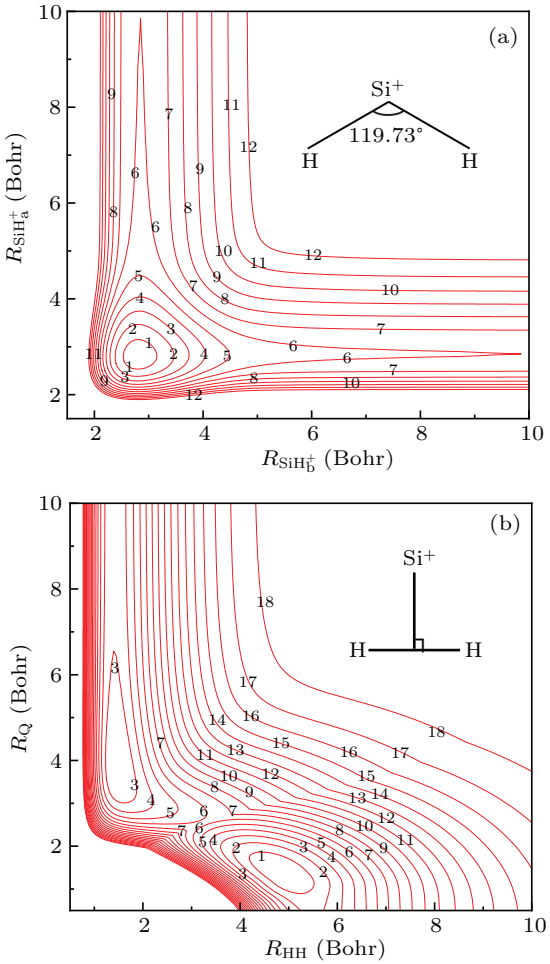


Fig. 1. Equipotential contour plot (a) for the structure of global minimum value in which the angle $\angle[HSiH]^+ = 119.73°$, contours are equally spaced by 0.4 eV, starting at −5.1 eV and (b) for the Si^+ ion approach to H_2 molecule in C_{2v} symmetry, contours are equally spaced by 0.4 eV, starting at −5.1 eV.

Table 2. The spectroscopic parameters of stationary points.

	R_{HH} (Bohr)	$R_{SiH_a^+}$ (Bohr)	$R_{SiH_b^+}$ (Bohr)	θ (°)	ω_{sym} (cm^{-1})	ω_{bend} (cm^{-1})	ω_{asym} (cm^{-1})
Global minimum							
This work	4.8400	2.8008	2.8008	119.73	2170.96	718.676	2256.92
Theo.[16]	4.820	2.806	2.806	118.38	2244.11	1247.92	2265.65
Theo.[32]	4.7979	2.802	2.802	119.70	2268	966	
Theo.[12]	4.8776	2.8161	2.8161	120			
Theo.[15]	4.8455	2.8008	2.8008	119.77	2189.7	912.6	2267.1
Exp.[10]	4.8529	2.8161	2.8161	119			
Local minimum							
This work	1.480	3.842	3.842	22.21	3838.43	509.20	909.01
Theo.[16]	1.481	3.821	3.821	22.35	3742.25	300.60	894.77
Transition state							
This work	3.232	3.007	3.007	65.01	1579.36	142.1i	1205.17
Theo.[16]	2.999	3.041	3.041	59.08	1353.76	1511.80i	1124.90

In order to find the reason why present PES and Gao's PES are so different in the transition state, Fig. 2 shows the potential energy curves of Si^+ ions close to the midpoint of H_2 under C_{2v} symmetry when the bond length of H_2 is fixed at 2.999 Bohr and 3.232 Bohr. To compare conveniently, the *ab initio* values and the results obtained from Gao's PES are

also displayed in Fig. 2. Clearly, there is a conical intersection between the ground state ($1^2A'$) and excited state ($2^2A'$) and present PES gives a correct description of the conical intersection. However, the potential energy curves obtained from Gao's PES obviously cannot correctly describe the conical intersection. We suppose this may be attributed to the drawback of many-body expansion method.

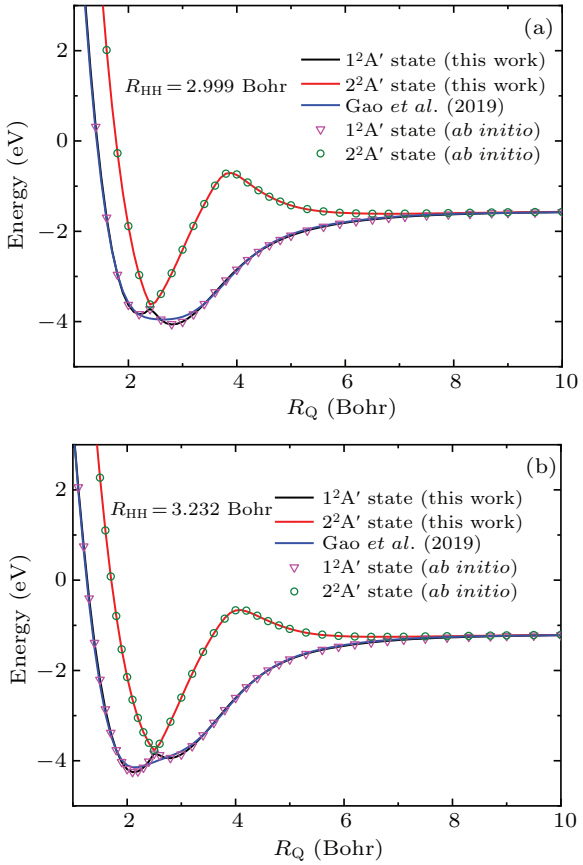


Fig. 2. The potential energy curves for the Si^+ ion approach to the midpoint of H_2 molecule at C_{2v} symmetry along with the *ab initio* results and the values obtained from Gao's PES[16] ((a) for $R_{HH} = 2.999$ Bohr, (b) for $R_{HH} = 3.232$ Bohr).

Figure 3(a) shows the change of potential energy for the Si^+ ion moves around the H_2 molecule as the bond length of H_2 fixed at 1.401 Bohr. As seen in the figure, there is a potential well with depth of about 0.4 eV at the position $R_Q = 4$ Bohr, and $\theta = 90°$. Figure 3(b) exhibits the H atom moving around SiH+ ion as $R_{SiH^+} = 2.844$ Bohr. Obviously, there is a shallow potential well and a deep potential well on the side of H atom and Si^+ ion, respectively. The deep well is located at $R_Q = 3.8$ Bohr, $\theta = 40°$ with the depth about 2.7 eV and the shallow well is located at $R_Q = 1.2$ Bohr, $\theta = 135°$ with the depth about 0.9 eV.

Figure 4 displays the minimum energy paths of the PES at several selected angles. As seen in the figure, the energy of $Si^+ + H_2$ asymptote is set to be zero. It is very clear that the $Si^+ + H_2 \rightarrow SiH^+ + H$ reaction is highly endothermic and the endoergic energy is about 1.30 eV when zero-point energy is not considered. As seen in the figure, there is a shallow potential well and a deep potential well on both sides of the barrier at 30°. The potential well on the right side gradually disappears with the increases of angle. The barrier decreases at first, then disappears, and then gradually increases with the increasing of angle. In the present work, the spin–orbit coupling effect is not considered since it has a little influence on the endothermic energy of the $Si^+ + H_2$ reaction.

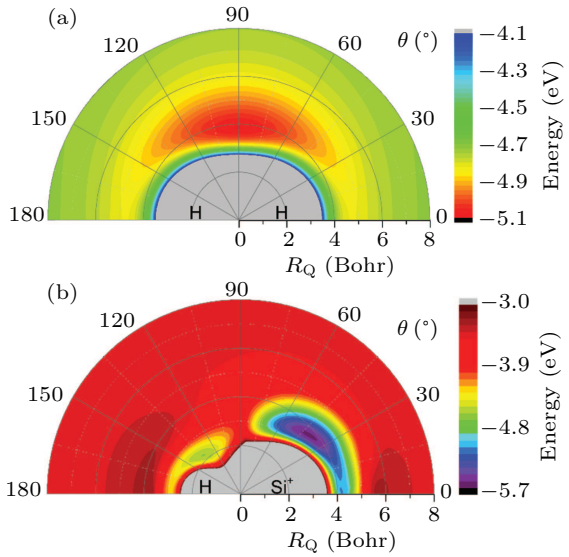


Fig. 3. (a) Color plot for the Si^+ ion moves around the H_2 molecule when the bond length of H_2 is fixed at 1.401 Bohr. (b) Color plot for H atom moves around SiH^+ ion when the SiH^+ bond length fixed at the equilibrium geometry.

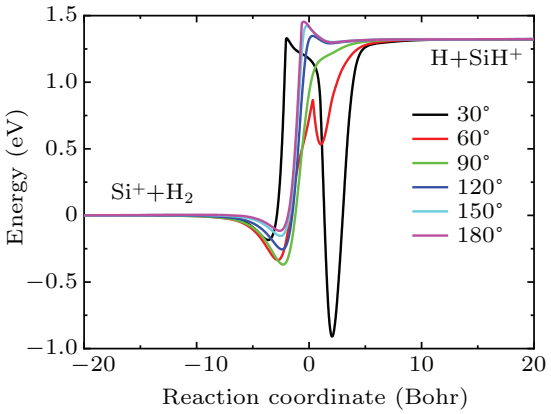


Fig. 4. The minimum energy paths of the new PES at different $[SiHH]^+$ angles.

3. Dynamics

Based on the newly constructed PES, the dynamics calculations of the $Si^+ + H_2 \rightarrow SiH^+ + H$ reaction was carried out by using time-dependent wave packet method, which is widely used in the reaction scattering calculation, such as K + H_2,[28] and Li + H_2.[29] As discussed above, the $Si^+ + H_2 \rightarrow SiH^+ + H$ reaction is highly endothermic with the energy about 1.3 eV. We suppose the reaction probability of initial state ($v_0 = 0, j_0 = 0$) will be very small, which is similar

with K + H_2 reaction.[28] Therefore, we chose ($v_0 = 2, j_0 = 0$) as the initial state. In the dynamical calculations, the convergence test should be carried out at first. In the present work, the convergence test is performed on the reaction probability of $J = 0$. Finally, the optimal parameters are obtained and shown in Table 1. As shown in Fig. 4, there is a deep well on the reaction path, therefore it is very time consuming. For reducing the computational cost, the reaction probabilities for particular J (e.g., 0, 10, 20, ..., 60) were computed and the others were obtained by using the J-shifting method.[33]

Table 3. Numerical parameters used in the TDWP calculations (atomic units unless otherwise stated).

Scattering coordinate	$R_{\min} = 0.50$, $R_{\max} = 17.0$
No. of grids in R	$N_R^{\text{tot}} = 179$, $N_R^{\text{int}} = 159$
Diatomic coordinate	$r_{\min} = 0.50$, $r_{\max} = 20.0$
No. of grids in r	$N_r^{\text{tot}} = 255$, $N_r^{\text{asy}} = 79$
No. of angular basis	$N_j = 130$
Initial wave packet	$\delta = 0.14$, $E_0 = 0.5$ eV, $R_0 = 13.0$
Total propagation time	$T_{\text{tot}} = 70000$, $\Delta_t = 10.0$
Absorbing potential	$C_{\text{a}}^R = 0.10$, $C_{\text{b}}^R = 0.08$, $C_{\text{a}}^r = 0.12$, $C_{\text{b}}^r = 0.30$ $n = n' = 2$, $R_{\text{a}} = 13.3$, $R_{\text{b}} = 16.8$, $r_{\text{a}} = 16.7$, $r_{\text{b}} = 19.9$

Figure 5 shows the ICSs of the title reaction in the collision energy range from 0 to 1.0 eV. As seen in the figure, a threshold about 0.19 eV is found which is consistent with Fig. 4 as the zero-point energy and vibrational energy considered. In addition, some resonance structures are found on the ICS curve, and this can be attributed to the deep well on the reaction path which support numbers of quasi-bound and bound states. The ICSs increase with the increasing collision energy, which is similar with other endothermic reactions.

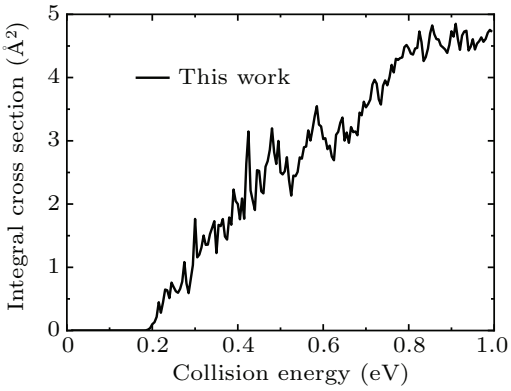


Fig. 5. The integral cross sections of the $Si^+ + H_2$ ($v_0 = 2, j_0 = 0$) → $SiH^+ + H$ reaction as a function of collision energy.

The rate constants of the initial state ($v_0 = 2, j_0 = 0$) are presented in Fig. 6 in the temperature range from 333 K to 1000 K. As shown in the figure, the rate constant increases with roughly a factor about 20 with the increase of temperature. We suppose the rate constants of SiH_2^+ system will be helpful for the modeling of star atmospheres.

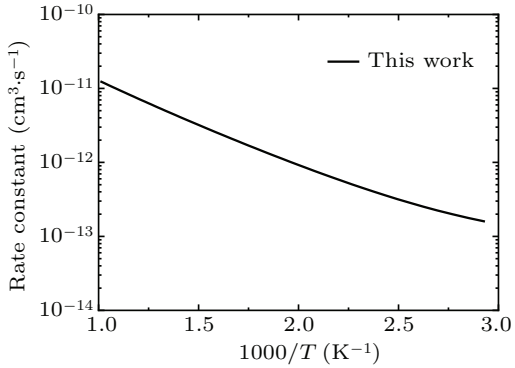


Fig. 6. The rate constants of the $Si^+ + H_2$ ($v_0 = 2, j_0 = 0$) → $SiH^+ + H$ reaction in the temperature range up to 1000 K.

4. Conclusions

Based on 18223 *ab initio* points, the global PES of the SiH_2^+ system was constructed by using PIP-NN method. The properties of the new PES are discussed and compared in detail with previous theoretical and experimental data. The spectroscopic constants obtained from the new PES are in good agreement with experimental and previous theoretical results. In addition, present PES is in general better than previous ones, and especially the new PES gives a correct description in the region around the conical intersection. To verify the validity of the new PES, the dynamics calculations of the $Si^+ + H_2$ ($v_0 = 2, j_0 = 0$) → $SiH^+ + H$ reaction is studied by using the TDWP method. The dynamics properties such as ICSs and rate constants are reported in this work. In conclusion, the new PES of the SiH_2^+ system shows reasonable and accurate behavior over the configuration space studied.

Acknowledgement

Project was supported by Key Projects of Science and Technology in the 13th Five Year Plan of Jilin Provincial Department of Education, China (Grant No. JJKH20200482KJ).

References

[1] Armentrout P B 2000 *Int. J. Mass Spectrom.* **200** 219
[2] Ng C Y 2002 *J. Phys. Chem. A* **106** 5953
[3] Zanchet A, Godard B, Bulut N, Roncero O, Halvick P and Cernicharo J 2013 *Astrophys. J.* **766** 80
[4] Li W T, Yuan J C, Yuan M L, Zhang, Y, Yao M H and Sun Z G 2018 *Phys. Chem. Chem. Phys.* **20** 1039
[5] Koseki S and Gordon M S 1987 *J. Mol. Spectrosc.* **123** 392
[6] Escribano R and Campargue A 1998 *J. Chem. Phys.* **108** 6249
[7] Kasap S and Capper P 2017 *Springer Handbook of Electronic and Photonic Materials* (Heidelberg: Springer) pp. 573–576
[8] Grevesse N and Sauval A J 1970 *Astron. Astrophys.* **9** 232
[9] Sauval A J 1969 *Solar Phys.* **10** 319
[10] Curtis M C, Jackson P A, Sarre P J and Whitham C J 1985 *Mol. Phys.* **56** 485
[11] Hirst D M and Guest M F 1986 *Mol. Phys.* **59** 141
[12] González M, Sayós R, Mota F and Aguilar A 1987 *Chem. Phys.* **113** 417
[13] Mort S P, Jennings N A and Balint-Kurti G G 1994 *Chem. Phys. Lett.* **222** 603

[14] Mort S P, Jennings N A, Balint-Kurti G G and Hirst D M 1994 *J. Chem. Phys.* **101** 10576

[15] Bauer C, Hirst D M, Hall D I, Sarre P J and Rosmus P 1994 *J. Chem. Soc. Faraday Trans.* **90** 517

[16] Gao F, Zhang L L, Zhao W L, Meng Q T and Song Y Z 2019 *J. Chem. Phys.* **150** 224304

[17] Zhao W L, Tan R S, Cao X C, Gao F and Meng Q T 2021 *Chin. Phys. B* **30** 123403

[18] Werner H J, Knowles P J, Knizia G, Manby F R and Schütz M, *et al.*, MOLPRO, version 2012.1, a package of *ab initio* programs, 2012, see http://www.molpro.net

[19] Schuchardt K L, Didier B T, Elsethagen T, Sun L, Gurumoorthi V, Chase J, Li J and Windus T L 2007 *J. Chem. Inf. Model.* **47** 1045

[20] David F 1996 *J. Comput. Chem.* **17** 1571

[21] Pritchard B P, Altarawy D, Didier B, Gibson T D and Windus T L 2019 *J. Chem. Inf. Model.* **59** 4814

[22] Werner H J and Knowles P J 1988 *J. Chem. Phys.* **89** 5803

[23] Werner H J and Knowles P J 1985 *J. Chem. Phys.* **82** 5053

[24] Knowles P J and Werner H J 1985 *Chem. Phys. Lett.* **115** 259

[25] Jiang B, Li J and Guo H 2016 *Int. Rev. Phys. Chem.* **35** 479

[26] Jiang B and Guo H 2013 *J. Chem. Phys.* **139** 054112

[27] Li W T, He D and Sun Z G 2019 *J. Chem. Phys.* **151** 185102

[28] Li W T, Wang X M, Zhao H L and He D 2020 *Phys. Chem. Chem. Phys.* **22** 16203

[29] Yuan J C, He D and Chen M D 2015 *Phys. Chem. Chem. Phys.* **17** 11732

[30] Huber K P and Herzberg G 1979 *Molecular Spectra and Molecular Structure. IV. Constants of Diatomic Molecules* (Van Nostrand Reinhold, New York)

[31] Carlson T A, Copley J, Duric N, Elander N, Erman P, Larsson M and Lyyra M 1980 *Astron. Astrophys.* **83** 238

[32] Dyke J M, Jonathan N, Morris A, Ridha A and Winter M J 1983 *Chem. Phys.* **81** 481

[33] Zhang D H and Zhang J Z H 1999 *J. Chem. Phys.* **110** 7622